INTERNATIONAL CENTER FOR NUMERICAL METHODS IN ENGINEERING

Development and Characterization of Semitransparent Double Skin PV Façades

J. Cipriano
C. Lodi
D. Chimisana
G. Houzeaux
O. Perpiñan

Publication CIMNE Nº-324, October 2008

Development and Characterization of Semitransparent Double Skin PV Façades

J. Cipriano
C. Lodi
D. Chimisana
G. Houzeaux
O. Perpiñan

Publication CIMNE Nº-324, October 2008

International Center for Numerical Methods in Engineering
Gran Capitán s/n, 08034 Barcelona, Spain

EUROSUN 2008
1st International Congress on Heating, Cooling, and Buildings
7th to 10th October, Lisbon - Portugal

156 - Development and characterization of semitransparent double skin PV façades

J.Cipriano[1*], C. Lodi[2], D.Chemisana[3], G.Houzeaux[4], O. Perpiñán[5]

[1] CIMNE-BEEGroup, Building Energy and Environment Group. International Centre for Numerical Methods in Engineering. Dr. Ullés nº 2. 3º. 08224. Terrassa. Spain.

[2] University of Lleida (UdL). CIMNE-MACS Clarssroom. Pere de Cabrera s/n. CREA Building. Cappont Campus. 25001. Lleida. Spain

[3]University of Lleida (UdL). Solar Energy and Building Physics Group. Pere de Cabrera s/n. CREA Building. Cappont Campus. 25001. Lleida. Spain

[4]Barcelona Supercomputing Centre (BSC-CNC)- Department of Computer Applications in e-Science & Engineering. Nexus II Building. Jordi Girona, 29. 08034 Barcelona .Spain.

[5]ISOFOTON - Montalbán, 9. 28014 Madrid.

[*] Jordi Cipriano, cipriano@cimne.upc.edu

Abstract

This research aims at developing new standardized typologies of semitransparent double skin façades formed by PV laminates in the outer skin. At present there are many buildings in Europe which incorporate such active façades, but all have been designed as user defined projects and very few accurately evaluate the feasibility of using the heat produced within the air gap. There is actually a lack of effective methodology to allow non-specialist architects to design and evaluate such façades. This research tries to address this situation: the Spanish PV manufacturer ISOFOTON, together with the partners of the PVTBUILDING project: CIMNE, the UdL, PICH-Aguilera, DOMUS and BSC have begun a collaboration to design industrialized modules constituted by an external semitransparent PV layer, a wide air gap and an internal glass layer. This paper describes the results of four stages of a more wide research: a detailed analysis of the existing double skin façades in office buildings and the definition of a family of standard PV modules and ventilated façades; an intensive evaluation of the existing heat transfer relations for asymmetrical heated vertical air channels; the programming of a dynamic transient solver based on TRNSYS and the validation of the codes with the set up of prototypes and the beginning of an experimental campaign.

Keywords: PV/Thermal, ventilated double skin façades, heat recovering

1. Introduction

In recent years many authors have been working in the field of double skin ventilated façades. Since the 1990's the Joint Research Centre has been carrying out an intensive characterization of PV ventilated façades, with and without ventilated air gaps. Some European funded projects have been actively supporting this work, PASSLINK, PV-HYBRIDPAS and IMPACT [18]. Between 1999 and 2000, the Centre for Applied Research at the University of Applied Sciences Of Stuttgart [7,11] undertook the theoretical analysis and monitoring of the Mataro's public library building, which had the first PV ventilated façade in Europe. More recently, the treatment of the induced flow and the heat transfer at the air gap and the surfaces of a natural ventilated double skin façade has been progressively refined by Brinkworth [3,4]. Concerning to the mathematical model to define the energy performance

of such façades, sophisticated models for double skin façades were developed by Saelens [15]. Although these detailed studies have lead to an increase in the knowledge of the heat transfer processes, there are still many unclear fields such as: the convective heat transfer coefficients definition; the evaluation of the direct solar radiation absorbed by the solid parts; the evaluation of the mass flow rate in non-developing turbulent flows and, the coupling with the HVAC systems.

Concerning to the dissemination of the PV ventilated façades, many recent newly constructed office buildings have included such devices in their designs; however, the spread of this technology has not occurred at the necessary scale. One of the reasons, we believe, has to do with the lack of standardised designs which forces the designers to select the glass transparent surfaces and the support structures separately from the PV laminates, leading to fitting problems and size incompatibilities.

2. Definition of new modules and standardized façades

At present, ISOFOTON manufactures PV modules which are clearly optimised for PV electricity production, looking for a maximum relation between the number of PV cells and the overall surface of the module (packing factor). These PV modules, however, are not well suited for PV integration in transparent office buildings, where transparency is also a crucial aspect. Trying to find a balance between electricity production and transparency, ISOFOTON will manufacture 4 new PV modules made of glass-glass and glass-Tedlar (see figure 1).

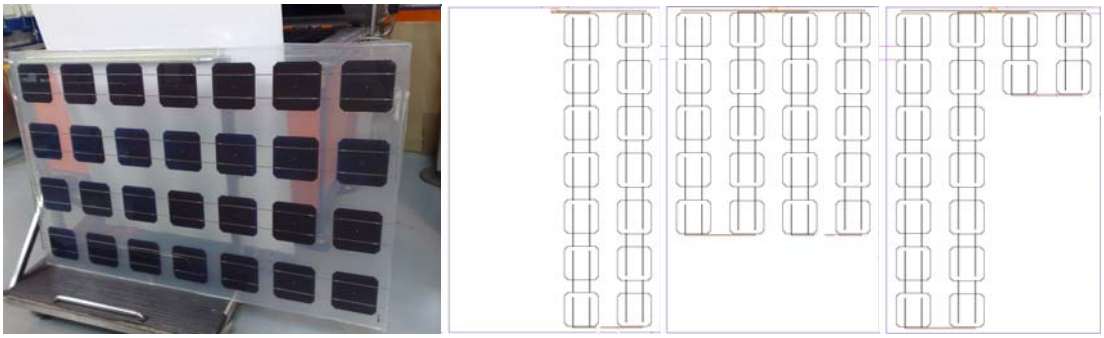

Fig. 1. PV modules made for building integration. Size:98.2 x 151.5 cm. PV Cells size: 15.6 x 15.6 cm.

During the developing phase, the main requirements of a first standardized PV ventilated façade typology were defined: the façade should start at the first floor of the building because the ground floor usually presents a different design; the width of the air gap must range between 40 and 60 cm to allow an easy maintenance and the inlet grille will be placed horizontally at the bottom of the façade while the outlet grille will be placed vertically and formed by motorized blinds. In the summer, the connection with the HVAC system will be closed and the façade will work only in free convection mode to improve the thermal resistance of the space in contact with. In winter, the façade will act as a pre-heating system, coupled to the HVAC system.

3. Numerical analysis of the heat transfer coefficients in laminar free convection

Many authors have made analysis of cavities or ventilated façades under buoyant flows. However they are all limited to laminar symmetric boundary conditions. Within this research a methodology based on

Reynolds Averaged Navier Stokes (RANS) CFD simulations is used over laminar and asymmetric flows. The main scope is to obtain reliable correlations for $\overline{Nu}$ and for the mass flow rate.

3.1. Validation of the CFD hypothesis for the laminar situations

A wide number of simulations have been carried out (381); some of them have been used to validate the CFD model and the numerical assumptions with experimental results and previous authors. In the case of laminar situations, maximum deviations of 10 % have been obtained in the prediction of average Nusselt numbers and mass flow rate. In figure 2, a comparison between the numerical values of $\overline{Nu}$ and the mathematical expressions of different authors is showed [1,13,14].

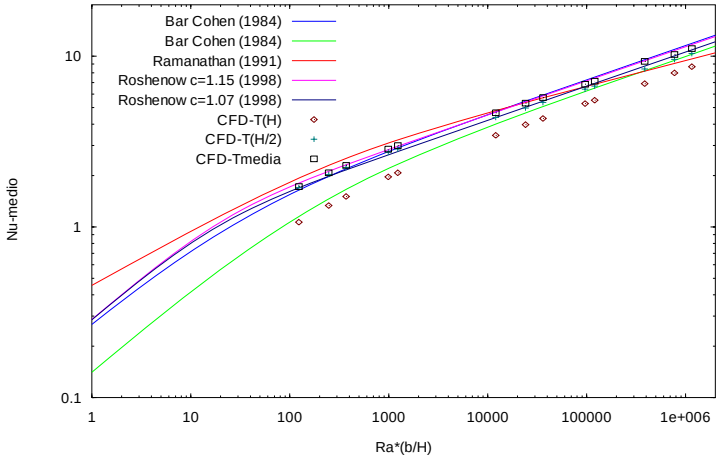

Figure 2. Comparison of $\overline{Nu}$ for symmetric uniform wall heat fluxes

3.2. New correlations for $\overline{Nu}$ and mass flow rates

Using the CFD simulations and applying a non linear regression based on iterative estimation algorithms (through the SPSS software) different correlations for the cases with asymmetric isofluxes have been obtained. In the case of the Nusselt numbers, the new correlations are based on the expressions of Bar-Cohen and Roshenow [1], but including the effect of the asymmetry (q_{wc} / q_{wh}), being q_{wc} and q_{wh}, the hot and cold wall isofluxes respectively:

$$\overline{Nu}_{h,\overline{T}_w} = \left(\frac{12}{Ra''_{qh}} \left(\frac{q''_{wc}}{q''_{wh}} \right) + \frac{6}{Ra''_{qh}} \left(1 - \frac{q''_{wc}}{q''_{wh}} \right) + \frac{1.88}{\left(Ra''_{qh} \right)^{0.4}} \right)^{-0.5} \quad (1)$$

$$\overline{Nu}_{c,\overline{T}_w} = \left[\frac{12}{Ra''_c} \left(\frac{q''_{wh}}{q''_{wc}} \right)^{-0.167} + \frac{1.88}{\left(Ra''_c \right)^{0.37}} \right]^{-0.548} \quad (2)$$

Where: $\overline{Nu}_{h,\overline{T}_w}$ is the average Nusselt number for the hot wall; $\overline{Nu}_{c,\overline{T}_w}$ is the average Nusselt number for the cold wall. In the case of the mass flow rate, a new correlation for the friction factor has been obtained:

$$f_{app}\,Re = 96 + \frac{0.7311}{H^{+}}\left(\frac{q''_h}{q''_c}\right)^{0.4067} \quad (3)$$

A comparison of these three correlations with the numerically calculated results has shown deviations lower than 6 %. However, some refinements in the equation 2 for situations with low Rayleigh numbers and in equation 3 for high asymmetric cases will be carried in the next future.

4. Dynamic transient models for the energy evaluation

Three TRNSYS types have been programmed to define the façade energy performance: the PV laminate type, the air channel type and the rear glass type. All the types are dynamically coupled by the TRNSYS sequentially solver: the heat conduction heat sources obtained from the first and third types are transferred to the second type as a Newmann boundary condition. Once the heat transfer coefficients, the mass flow rate and the average wall temperatures are obtained within this type, they are returned back to the first and third type. This is an iterative process which converges each time step. The underlying mathematical and physical models are described in the sections bellow.

4.1. Physical model

Air enters the façade at the bottom opening with an average inlet temperature ($T_{f,i}$) which is assumed equal to the uniform exterior air temperature (T_o). Hot air exits from the top of the chimney at outlet average temperature ($T_{f,o}$). The following heat transfer processes simultaneously happens within the façade: solar radiation absorbed by the S_g lid layers, thermal radiation between the back side of the PV laminate and the rear glass front side, thermal radiation between the external layer of the PV laminate and the sky and heat convection between the exterior, the interior and the façade.

4.2. Heat conduction transfer within the semitransparent PV laminate and the rear glass

The semitransparent PV laminate has three layers: the exterior layer is clear glass, the middle layer is formed by the PV cells and EVA in the spaces among them, and the third layer can be translucent Tedlar or glass, depending on the typology. The rear glass varies from a single glass in the simplest case, to a triple glaze. The governing equation and the boundary conditions within each layer are:

$$\begin{aligned} &\rho c_p \frac{\partial T}{\partial t} - \nabla \cdot (k \nabla T) = Q \\ &T = T_e \qquad in\ x = e_{PV} \\ &k \nabla T \cdot n = \bar{h}_{co}(T_o - T_c) + h_{rcs}(T_s - T_c)) \quad in\ x = 0 \end{aligned} \quad (4)$$

Where: ρ is the density of each layer (Kg/m^3); c_p is the specific heat coefficient (J/KgºK); T is the temperature of the layer (ºK); k is the thermal conductivity (W/mºK); Q is the volumetric heat source (W/m^3), T_e is the temperature of the last node (ºK); T_c is the temperature of the first node (ºK); T_s is the radiative sky temperature (ºK); $\bar{h}_{co}$ is the average convection heat transfer coefficient between the PV and the exterior (W/m^{2o}K); h_{rsc} is the radiation heat transfer coefficient (W/m^{2o}K) and e_{pv} is the thickness of the PV laminate (m). Equation 4 is solved using a finite element scheme in one dimension. The temporary term is discretized using the trapezoidal rule. By deriving the weak form of Equation 4 and applying the Galerkin method, we can obtain a discretized system of equations defined as:

$$[A]\cdot\left[T^{n+\theta}\right]=\left[r^{n+\theta}\right] \quad (5)$$

Where: [*A*] is the coefficients array; [$T^{n+\theta}$] is temperatures vector at time step=$n+\theta$; [$r^{n+\theta}$] is the residual array; *n* is the time step number; θ is the temporal coefficient. When $\theta=1$, the backward Euler scheme is used and when $\theta=1/2$ the Crank-Nicolson scheme is used. The array [*A*] is three-diagonal. The values of the terms in each array depend on the layer. The physical properties of the second layer of the PV laminate (PV cells and EVA) are affected by the packing factor (*P*). In the case of the rear glass, the FEM discretization will be the same as the PV laminate, but the boundary conditions will be the opposite (Dirichlet at $x=0$ and Newmann at last node). The system of equations in both domains is solved using a direct three-diagonal algorithm (TDMA). Once the temperatures of each node are obtained, the conduction heat flux towards the air channel $q''_{e,cond}$ and $q''_{g1,cond}$ are computed using Fourier's law.

4.3. Air channel mass flow rate and average temperatures

The air channel is modelled through a stationary one-dimensional volume, with a linearly temperature variation in the vertical direction. Three different working conditions are possible: $q"_{ef} = q"_{g1f}$; $q"_{ef} \neq q"_{g1f,}$ and adiabatic condition $q"_{ef}$; $q"_{g1f} = 0$. Concerning the nature of the flow, three situations are considered: natural, forced (wind or mechanical fan) and mixed convection. In the natural convection situation, two flow regimes exist: the laminar and the turbulent. Besides, a distinction between thin and wide channels is considered. The governing equation, once integrated, can be expressed as:

$$\dot{m}c_p\left(T_f - T_{f,i}\right)=\left(q''_{ef} + q''_{g1f}\right)Wy \quad (6)$$

Where: T_f is the air average temperature at height *y* (ºK); *y* is the height (m); $T_{f,}$ is the average temperature at the inlet (ºK); $\dot{m}$ is the mass flow rate (Kg/s); *W* is the width of the façade (m) and $q"_{ef}$ and $q"_{g1f}$ are the convective heat sources. They are calculated as: $q''_{ef} = q''_{e,cond} - q''_{reg}$ and $q''_{g1f} = q''_{g1,cond} + q''_{reg1}$. Assuming the Newton law of cooling for the heat convection sources, making some arrangements and integrating along the façade height we can obtain the average wall and outlet temperatures.

The flow-rate is obtained by equating the sum of the pressure differences which drive the flow (wind and buoyancy) with that of those opposing it (hydraulic and friction losses):

$$A\cdot\left(H^+\right)^3 + B\cdot\left(H^+\right)^2 - \frac{1}{2}\left[\left(f_{app}\,Re_{Dh}\right)\cdot H^+ + \sum K_h\right]=0 \quad (10)$$

where: $H^+ = \dfrac{H}{2\,Re_{Dh}\,b}$ is the dimensionless height; $A = \dfrac{2SGr_{Dh}}{Pr}$ is the buoyancy term; $B = \dfrac{\Delta P_w D_h{}^4}{\rho\nu^2 H^2}$ is the wind-induced term; *S* is the stratitification coefficient; K_h are the inlet and outlet hydraulic losses; f_{app} is the apparent friction factor and D_h is the hydraulic diameter (m). The term $f_{app}Re$ is likewise depending on H^+, which means that an iterative process must be set up. The expression of $f_{app}Re$ depends on the boundary conditions, on the flow nature, and on the flow situation: in laminar free convection and symmetric uniform heat fluxes, the correlations of Kakaç [9] were validated through CFD simulations. In the case of adiabatic wall boundary conditions, the correlations of Kakaç [9] are also accepted if $Gr_D < 10^5$. In the case of asymmetric conditions, the new correlation

(see equation 3) is used. In turbulent free convection, the term $f_{app}Re$ is no longer linear dependent on H^+. For this situation only correlations for forced turbulent fully developed flow exist [6]. In mixed flow convection, a composition of the previous correlations will be used. The pressure difference term (ΔP_w) is calculated using a dynamical pressure expression dependent of the pressure coefficients.

Once all the terms are determined, a Newton Raphson method is used to solve Equation 10.

4.4. $\overline{Nu}$ correlations for the air gap and the rear glass

The average convection heat transfer coefficients are derived from the Nusselt numbers ($\overline{Nu}$). In laminar free convection flows the $\overline{Nu}$ is obtained through different correlations: in the case of symmetric uniform heat fluxes the correlation of Roshenow with c=1.15 [14] is used, in the case of asymmetric uniform heat fluxes the new correlations obtained in this research (equations 1 and 2.) are used for hot and cold walls. In turbulent free convection flows, in the case of wide channels, the correlation of Churchill [5] is used. In forced convection flows, a distinction between developing and fully developed flows is made. In case of laminar developing flows, the correlations of Bejan [2] and Kays [10] are used. In case of laminar fully developed flows, the $\overline{Nu}$ are constants. In case of turbulent developing flows, a correlation obtained by Saelens [15] is used. Concerning to the turbulent developed flows, the equations of Kays [10] are also valid.

In the case when the rear glass is formed by multiple glass layers, the equations and correlations obtained for air cavities will be used.

4.5 Convection heat transfer between the exterior, the interior and the façade

The convection heat transfer between the glass layer of the PV laminate and the exterior follows the Newton's law of cooling. In 1984, Sharples [16] concluded that the linear correlations obtained for solar collectors, are also valid for ventilated facades. The convective heat transfer between the last layer of the rear glass and the room also follows the Newton law of cooling but the convective heat transfer coefficient is affected by the HAVC system of the building.

4.6 Thermal and Solar radiation. Spectral and angular dependency

The semitransparent PV laminate is divided in two equivalent surfaces: the opaque surface, formed by the sum of the PV cells surfaces and the semitransparent surface, which is the sum of the transparent spaces of the PV module.

The opaque surface has an external glass layer, the EVA layer and the PV cells. The product tau-alpha ($\tau\alpha$) is the optical property to be determined. The angular dependence was deeply analysed by Parretta [12] who concluded that an equivalent refractive index, higher than the glass refractive index, must be used. Since reflection at the interface EVA/PV cell is diffuse, the PV absorptance will be independent from the incidence angle and the angular dependence will only affect the transmittance of the glass and EVA joint. The incidence angle modifier (IAM_{PV}) will be used. This *IAM* will be obtained, for the beam radiation, using Fresnel equations of the air/glass interface.

In the semitransparent equivalent surface an overall hemispherical value has been obtained from the spectral dependency of each layer (glass, EVA and Tedlar). The optical properties of the rear glass are obtained from the TRNSYS database. The angular dependence must include the reflections between the semitransparent surfaces, thus, the net radiation method [17] will be used.

The thermal radiation between the semitransparent surface and the rear glass; between the last layer of the rear glass and the adjacent room and the radiation between the glass of the PV laminate and the sky is determined by solving the net heat transfer between two infinite grey surfaces.

4.7. Electricity generated by the PV

The electricity generated by the PV cells must be expressed as:

$$q''_e = (\tau\alpha)_n \, IAM_{PV} \, G_t \, P \, \eta_{PV} \qquad (\mathrm{W/m^2}) \qquad (10)$$

where: η_{PV} is the PV efficiency. The PV efficiency is depending on the PV cells temperature and on the incident radiation. To consider these two factors, a linear variation model has been adopted.

5. Prototypes and monitoring strategy

A distinction should be made between the determination of the energy efficiency at component/façade level and at building level. For this reason, the experimental activity will be divided in two stages and two different prototypes will be constructed. The first stage consists in the construction of a small system, very similar to TRE [8], formed by a single PV module tested under forced convection situations. The 8 new modules of ISOFOTON will be tested to obtain specific data about heat exchange and electricity performance. The second stage will be the construction of a more sophisticated system to test the best configuration of PV module under real conditions. This phase will start using the test cells of the Politecnico of Torino and later, the construction of similar cells in Lleida will be carried out. During August and September 2008 the monitoring task will start and it will be extended until the end of 2009. In the figure 3 the schemes for the first prototype are shown.

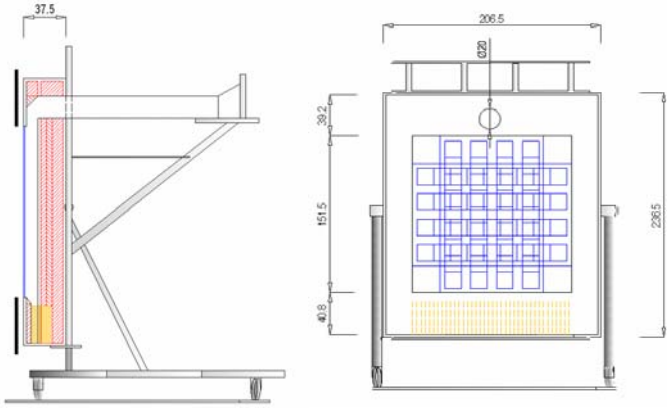

Fig.3. PV Schemes of the first prototype at the ITL in Lleida. Cross section and front view.

6. Conclusions

A strong thermodynamic coupling exists between the air flow through the naturally ventilated double-skin façade and the air temperature difference between the cavity and the outside. This interaction can only be predicted by sophisticated building energy modelling and simulation techniques as was done in the current study. Three new TRNSYS types have been developed and validated through numerical experiments. One first prototype has been constructed at the University of Lleida and the monitoring

period has just started. Experimental results to validate the TRNSYS types and to get some conclusions about the 8 new PV modules are expected to be available by the middle of 2009.

Concerning to the convective heat transfer and the mass flow rate within the air gap, this research has showed that there is still a lot of work to be done to clearly define the performance under transient turbulent free convection.

The first standardized typologies defined within this research will be further refined and included in the second prototype. Once they are validated under real conditions, the manufacturing process as well as the commercial strategy will be defined.

References

[1] Bar-Cohen A. and Rohsenow W.M. 1984. 'Thermally optimum spacing of vertical, natural convection cooled, parallel plates'. Journal of Heat Transfer. 106.
[2] Bejan A. and Kraus D. 2003. 'Heat Transfer Handbook. John Wiley & Sons Ltd.
[3] Brinkworth B.J. 2000. 'A procedure for the routine calculation of laminar free and mixed convection in inclined ducts'. International Journal of Heat and Fluid Flow. 21.
[4] Brinkworth B.J. and Sandberg M. 2006. 'Design procedure for cooling ducts to minimise efficiency loss due to temperature rise in PV arrays'. Solar Energy. 80.
[5] Churchill S.W and Ozoe H. 1973. 'Correlations for forced convection with uniform heating in flow over a plate and in developing and fully developed flow in a tube'. Journal of Heat Transfer. 95.
[6] Filonenko G.K. 1954. 'Hydraulic resistance in pipes. Heat Exchanger Design Handbook. Teploenergetica Vol 1. Hemispher Publisher Corporation.
[7] Fux V. 2006. 'Thermal Simulation of ventilated PV Façades'. Loughborough University.
[8] Gandini, A. 2003. 'Analisi numerica delle facciate fotovoltaiche a doppia pelle'. Politec. di Milano.
[9] Kakaç S., R. Shah and W.Aung. 1987. 'Handbook of single-phase convective heat transfer'. Wiley.
[10] Kays W., Crawford M.and Weigand B. 2004. 'Convective Heat and Mass Transfer. McGraw Hill.
[11] Mei L., Infield D., Eicker U., and Volker F. 2003. 'Thermal modelling of a building with an integrated ventilated PV facade'. Energy and Buildings. 35.
[12] Parretta A., Sarno A., and Yakubu H. 1999. 'Non-destructive optical characterization of PV modules by an integrating sphere.: Part I: Mono-Si modules'. Optics Communications.161.
[13] Ramanathan S. and Kumar R. 1991. 'Correlations for natural convection between heated vertical plates'. Journal of Heat Transfer. 113.
[14] Rohsenow W., Hartnett J. and Cho Y. 1998. 'Hanbook of Heat Transfer. McGraw Hill.
[15] Saelens D. 2002. 'Energy Performance Assessment of single storey multiple-skin facades'. Katholieke Universiteit Leuven - Faculteit Toegepaste Wetenschappen.
[16] Sharples S. and Charlesworth P. 1998. 'Full-scale measurements of wind-induced convective heat transfer from a roof-mounted flat plate solar collector'. Solar Energy. 62 -2.
[17] Siegel R. 2002. 'Thermal Radiation Heat Transfer'.Taylor and Francis.
[18] Wouters P.and Vandaele L. 1994. 'The PASSYS services: summary report'. European Commission Publication No. EUR 15113 EN